Development and Characterization of a Low-Pressure Calibration System for Hypersonic Wind Tunnels

Del L. Green*, Joel L. Everhart†, and Matthew N. Rhode†
NASA Langley Research Center, Hampton, VA 23681

Minimization of uncertainty is essential for accurate ESP measurements at very low free-stream static pressures found in hypersonic wind tunnels. Statistical characterization of environmental error sources requires a well defined and controlled calibration method. A calibration system has been constructed and environmental control software developed to control experimentation to eliminate human induced error sources. The initial stability study of the calibration system shows a high degree of measurement accuracy and precision in temperature and pressure control. Control manometer drift and reference pressure instabilities induce uncertainty into the repeatability of voltage responses measured from the PSI System 8400 between calibrations. Methods of improving repeatability are possible through software programming and further experimentation.

Nomenclature

p	Pressure (psi)
Δp	Residual Pressure (psi)
A_i	Everhart Coefficients (V_0, A_1, A_2, A_3, A_4)
V_0	Offset voltage (Eqn. 2)
Z	Everhart's normalized voltage
V	ESP output voltage (Volts)
A	Temperature (ºF) influence effect
B	Pressure Direction influence effect
C	Module Range (psid) influence effect
D	Sample Rate (Hz) influence effect
E	Sample Period (sec.) influence effect
β_i	Factor influence coefficients
β_0	Grand average of responses
X_i	Factor magnitudes
X	Individual Values
R	Moving Range Values of X
$\overline{X}$	Mean of X or Subgroup Average
$\overline{R}$	Mean of the range values
$\overline{\overline{X}}$	Mean of $\overline{X}$ or Grand Average
NPL_X	Natural Process Limits of X
CL_X	Centerline and mean of the X
$UCL_{\overline{X}}$	Upper control limit of the $\overline{X}$
$CL_{\overline{X}}$	Centerline and mean of the $\overline{X}$
$LCL_{\overline{X}}$	Lower control limit of the $\overline{X}$
UCL_R	Upper control limit of the R
CL_R	Centerline and mean of the R
LCL_R	Lower control limit of the R
i	Incremental subscript

Introduction

Wind tunnels use many types of transducers to measure pressure. When many simultaneous pressure measurements are required at different locations, the Electronically-Scanned Pressure (ESP) transducers (Figure 1) offer many advantages including the low cost per pressure port and compact design of the multi-port modules. ESP's can be very accurate when

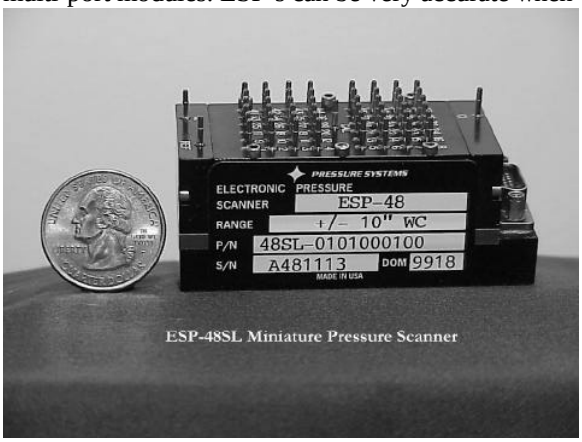

Figure 1.-ESP Transducer Module

used in controlled environments (i.e., when environmental sources of error are controlled). Temperature is understood to be a major time-dependent source of error during wind tunnel operation, causing transducers to shift away from the calibration response obtained at a different level of temperature. Some other possible error sources include, environmental pressure, magnitude, frequency, and direction of vibration, sample rate, sample period, settling time, module range and transducer over-pressurization. These temporal changes in the measurement system can be minimized by multiple calibrations made by rapid in-situ calibrations, an on-demand capability designed into the ESP system. However, inappropriate in-situ calibrations will increase the variance of the measurements because the calibration chases the normal variations found in the calibration standard

* Research Engineer, Student Member AIAA.
† Research Engineer, Senior Member AIAA.

and ESP transducer measurements, as discussed in general in "Evaluating the Measurement Process" (Wheeler and Lyday, 1984).

The use of ESP transducers in hypersonic wind tunnels has the additional complexity of very low pressure levels (free-stream static pressures typically near to 0.02 Psi). Wide pressure ranges must also be measured, approaching 50 psi at points on powered models. Thus, model pressures experienced during a tunnel run can vary over several orders of magnitude. Therefore, properly matching the module range to the orifice position on the model is critical to measure pressure accurately and to prevent over-ranging the transducer. Due to ESP module measurement uncertainty and changing flow characteristics such as shock wave movement and flow separations and impingements, it is challenging to place pressure ports in locations so that they will fall into an optimal zone for each range of module. Double tubing the pressure ports to multiple modules of different ranges is one solution to the problem. However, this can create a lag time problem relative to the single tubed ports at low pressure and it can substantially increase the cost of the model and the instrumentation, since additional data channels are required for the measurement. It also increases the complexity of model setup.

Another approach is to better characterize the uncertainties of the ESP modules at low pressures and minimize the large error sources, thus effectively extending the higher range modules to lower pressures. Two significant error categories are immediately obvious. The first is the calibration which was addressed by Everhart (1996). The second is the noise induced by environmental effects and the system itself.

The overall purpose of this study is to focus on the latter category to characterize the environmental, procedural, and instrument sources of error. This knowledge will allow the determination of whether the error sources need to be controlled or otherwise mitigated or whether they can be neglected. The study is divided into three phases. Phase I is a simple bench test designed to gather preliminary information about the ESP measurement system and to determine if the phenomena witnessed by Everhart (1996) is repeatable. In Phase II system stability will be determined as well as small scale studies conducted to answer key questions that may minimize the test time of the Phase III experiments. In Phase III, a full designed experiment will be conducted to characterize the environmental factors discussed above and determine if they significantly affect the variability of the measured voltages. Along with the characterization, the use of different calibration fitting functions will be further explored to assess calibration error.

The project is currently in its second phase with the calibration control system being the focus of a statistical process control (SPC) study to determine the control systems predictability. This paper presents an overview of the project, description of the calibration system, and results of a simple experiment exploring phenomena seen by Everhart (1996). The current results of the ongoing control system calibration using SPC will be discussed.

Dominant Error Sources

The three dominant contributors of uncertainty that limit the ESP modules are: (1) inaccuracies of the calibration curve, (2) uncertainties associated with reference pressure standard used for calibration, and (3) unstable environmental conditions. These contributors to uncertainty will be discussed below.

Calibration Curve

Inaccuracies of the calibration curve in low-pressure regions and curve dependencies on calibration pressure set point locations are significant sources of error (Everhart; 1996). The original Pressure Systems Inc. method used a parabolic curve through three calibration data points. The current method, also referred to as the standard method, is a five point calibration that fits a 4^{th} order polynomial curve to the data. Though the method allows some inflection in the calibration about zero differential pressure, the 4^{th} order calibration curves insufficiently characterize data taken within this region. Significant differences between the calibration data and regressed curve can occur near full scale due to mathematical deficiency of the fitting function. From a statistical standpoint, both calibrations are lacking because neither provides the necessary degrees of freedom for assessing pure error and lack-of-fit error as all degrees of freedom are used when determining the values of the fitting coefficients. Accordingly, the 4^{th} order curve coefficients can change for different subsets of calibration data drawn from the same over-sampled (more points than required for calibration) calibration data set as demonstrated in Figure 2a and 2b taken from Everhart (1996). Here, the complete calibration data set is represented by the open symbols, circles for the 0.36 psi modules and squares for the 2.5 psi modules. The pressure is plotted on a logarithmic scale versus the transducer voltage response. A standard-method calibration used the data subsets shown by the filled symbols. The curves illustrate the resulting calibrations obtained using these subsets. The differences (noted below) between Figures 2a and 2b are due solely to changing the point denoted as "cal set point." First, the extension of the curves is substantially different from the data's current trend beyond the range of the data. Second, the distribution

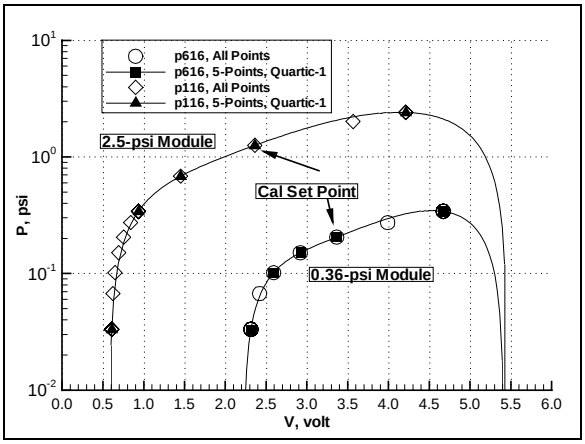

Figure 2a.-Effect of calibration pressure location on standard-method ESP calibration curve from Everhart; 1996

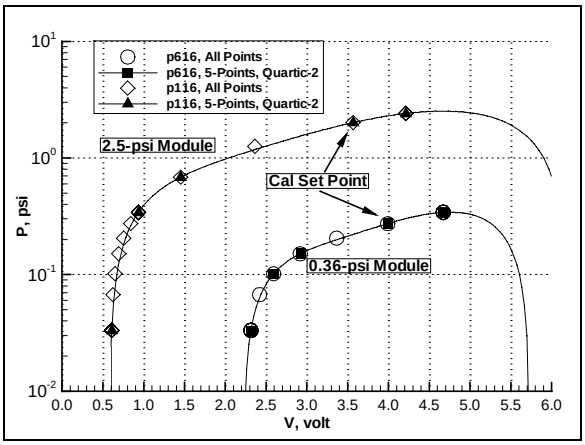

Figure 2b.-Effect of calibration pressure location on standard-method ESP calibration curve. Cont.

of points relative to the calibration curve is different depending on which data points were used to generate the curve. In other words, small changes in the calibration pressure selection can cause large changes in the corresponding response represented by the calibration curve. The differences between curve fit and data points are further highlighted in Figure 3a where the pressure, P, the pressure difference from the calibration curve, ΔP, and the magnitude of the percent reading error, ΔP/P, are plotted versus voltage for four different range ESP modules. These were determined using the standard method. At low pressures, actual pressure differences approaching 0.1 psi are realized, corresponding to a percent of reading error of 40%. These insufficiencies illustrate the need for an improved curve and a calibration procedure that provides enough degrees of freedom to evaluate uncertainty.

Everhart (1996) proposed a calibration curve form that better fit the calibration data. His formulation is given as:

$$p = A_1 Z^{\frac{1}{3}} + A_2 Z^{\frac{1}{2}} + A_3 Z + A_4 Z^2 \qquad (1)$$

where,

$$Z = V - V_0$$

Here, P is the pressure, A_1, A_2, A_3, and A_4 are the fitting coefficients, V is the transducer output voltage, and V_0 is the voltage at zero pressure. The coefficients are determined using a least squares fit of the entire data set. V_0 was determined iteratively as a part of the solution cycle for the A_i, instead of being measured directly. The improvements presented in

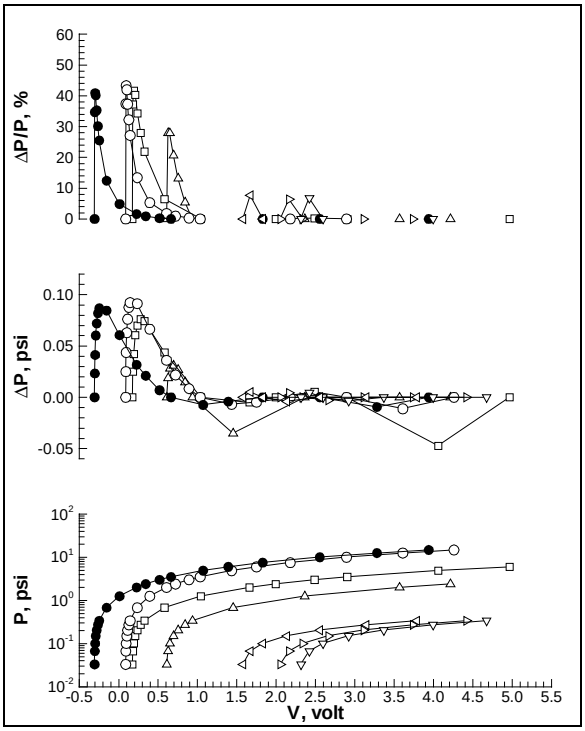

Figure 3a.-Standard ESP Quartic Fit curve from Everhart; 1996

Figure 3b (also taken from Everhart, 1996) are contrasted with those presented in Figure 3a. First, note the scale differences between Figure 3a and Figure 3b. The results presented in Figure 3b show considerable improvement via equation (1) compared to the standard ESP calibration curve using all data points, particularly for low-pressure use. Specifically, the pressure differences at low pressure have been reduced by an order of magnitude and the percent reading error has been reduced below 0.3% (neglecting error near zero). While much improved over the traditional polynomial fit, further improvements are desired at even lower pressures.

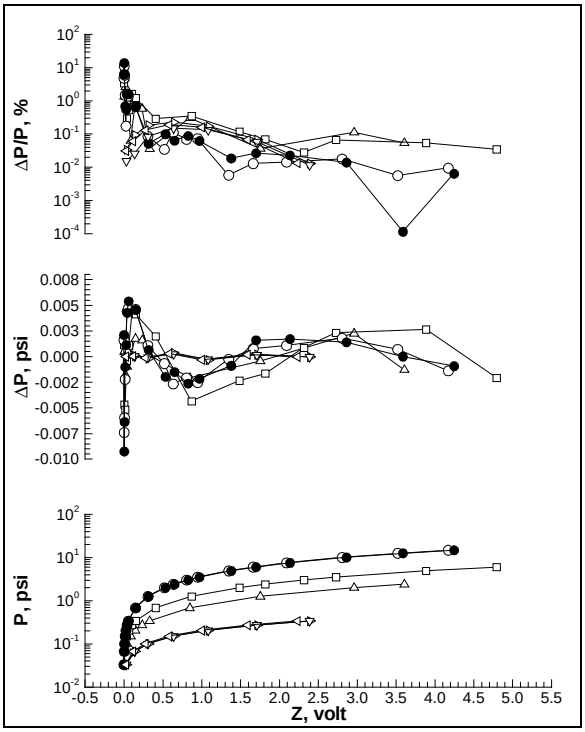

Figure 3b.-Everhart Calibration-Model Curve Fit from Everhart; 1996

Calibration Standard

Uncertainties related to the calibration pressure standard are another dominant source of error in the ESP system. The manufacturer-supplied 1-psia pressure calibration unit (PCU) uses a 5-psia Mensor pressure transducer (Model # 11998) with the output gain set to only look at the 0 to 1 psi range. PSI specifies the accuracy of the 1-psia PCU to be 0.02% of full scale (1 psi). The Operation Manual for Mensor Digital Pressure Gauge Model 11900 (1981) specifies the accuracy of the reference standard in the PCU to be 0.04% of full scale for a 90 day period if a zero adjustment has been conducted. The zero drift for this transducer is also 0.04% of full scale (5 psi) for a 90 day period and the span drift is 0.02% of full scale (5psi) for 90 days. It is understood that Mensor provided the best possible transducers of this series to PSI for use in the 1-psia PCU, therefore, the accuracy of the PCU is not in question. However, the Mensor transducer measurement accuracy is overshadowed by the zero and span drift and it lacks sufficient resolution to calibrate the ESP transducers in the low pressure range. The drift also has adverse affects on calibrations conducted using the 5-psia pressure calibration unit which uses the same transducer.

Environmental Conditions

Unstable environmental conditions also contribute to measurement uncertainty and they are particularly manifested at low pressure. These conditions (factors) include temperature, external pressure, and error due to vibration. Temperature effects are highly visible in the shift of V_0. External pressure affects the modules reference pressure by reducing leaks and will apply additional stresses to the ESP case and sensors. Errors due to vibration manifest in increased response variation and will depend on vibration frequency, amplitude, and transducer orientation. Design of Experiments (DOE) presented in detail in Montgomery (1997), and Myers and Montgomery (2002) and Statistical Process Control (SPC) methods, with details available in Wheeler and Chambers (1992), can be used to characterize and quantify the sources of error and determine the significance of contributing factors, including interactions between the factors which are unavailable in the traditional calibration scheme. DOE and SPC will be discussed and applied in subsequent sections of this paper where appropriate. Environmental contributions to measurement error may be many; however, only significant error sources need to be controlled, as the insignificant error sources will become an embedded part of the system noise.

Experimental Approach

A three phase program has been developed to characterize the environmental error sources of the ESPs. The first phase is a preliminary Design of Experiments (DOE) screening experiment that recreated and verified the calibration curve inaccuracies found by Everhart (1996). Phase II is composed of several smaller studies designed to address specific questions, such as the effect of set point order randomization on system calibration. This phase is also important to establish statistical stability upon which the experimental model for Phase III depends. Phase III uses all the pre-screening information gained in the first two phases to properly conduct a full designed experiment that characterizes the significant sources of error found in the ESP measurements. An important aspect of Phase III is that interaction effects can be identified and quantified. These phases are discussed in the following paragraphs.

Phase I- Simple Bench Test

DOE is a standard statistical method used to actively induce and quantify variation in a controlled manner which will maximize the information gained while conducting the minimum amount of experimentation necessary. The preliminary Phase I DOE screening experiment used a simple bench setup to perform a five-factor 2-level design. The five factors of interest chosen for this experiment were sample rate, sample period, module temperature, module range, and direction to which positive pressure is applied to the transducer (sample or reference side). These factors were tested at their low and high settings according to a statistically designed and randomized test matrix. An existing MKS calibration cart was used to set and measure the pressures (Figure 4). The calibration cart

is a dead end system that can only hold a needle valve controlled pressure as long as leaks permit,

Figure 4.-Phase I Experimental Setup

which is a very short period at low pressures, due to leakage found in pressure tubing connections and the ESP modules themselves. The pressures set during a calibration run ranged from 0.0225 psi to atmospheric pressure. A zero pressure data point was also taken with a hard (below 10^{-4} psi) vacuum being applied to both faces of the transducer. The run settings were held fixed over the prescribed schedule of pressure data points yielding a voltage response for each set pressure. Temperature was controlled by a Barocell heater mounted to an aluminum block in which the ESP modules are mounted. Experimental conditions were manipulated manually through redirecting the pressure lines and removing power from the Barocell heater.

The resultant calibration voltage responses for each run were fit using Everhart's functional form (Eqn. 1), producing the A_i coefficients. A second regression was then required to determine the influence levels of each studied factor and their interactions. Therefore, two regressions have been performed. The first is to determine the four calibration coefficients (A_1, A_2, A_3, and A_4) and the offset voltage (V_0) which are described in equation 1 and will be referred to as A_i. The second is conducted during the analysis performed by Design Expert analysis software (Stat-Ease, Inc.) to assess the influence that the factor variations had on the variability found in the A_i calibration coefficients.

The second regression assumes a linear model of factors and their interactions. In general, the empirical model for this regression is given by equation 2 as

$$A_i = \beta_0 + \sum_{A,B,\ldots,E} \beta_i X_i + \sum\sum_{i<j} \beta_{ij} X_i X_j + \sum\sum_{i\neq j\neq k} \beta_{ijk} X_i X_j X_k + \in \qquad (2)$$

where, β_0 is the grand average,

β_i are factor influence coefficients,

X_i are the factor levels.

The expanded model for the present case is shown in equation 3.

$$\begin{aligned} A_i = {} & \beta_0 + \beta_A A + \beta_B B + \beta_C C + \beta_D D \\ & + \beta_E E + \beta_{AB} AB + \beta_{AC} AC \\ & + \beta_{AD} AD + \beta_{AE} AE + \beta_{BD} BD \\ & + \beta_{CD} CD + \beta_{DE} DE + \beta_{ACD} ACD \\ & + \beta_{ADE} ADE \end{aligned} \qquad (3)$$

The factors A, B, C, D, and E were previously identified and defined as temperature, pressure direction, module range, sample rate, and sample period, respectively. The reader is referred to Myers and Montgomery (2002) for details of the implementation and application, and other statistical issues, such as factor aliasing and block designs. The effects of a given factor are estimated by adding the average of all responses at the high input value and subtracting the average of all responses obtained at the low input value. The effects of the influence factors and their interactions on the zero offset voltage V_0 are presented in Figure 5. Here, the half normal percent probability of the influence of each modeled effect is plotted versus the absolute value of the effect. The normal probability plot which will be

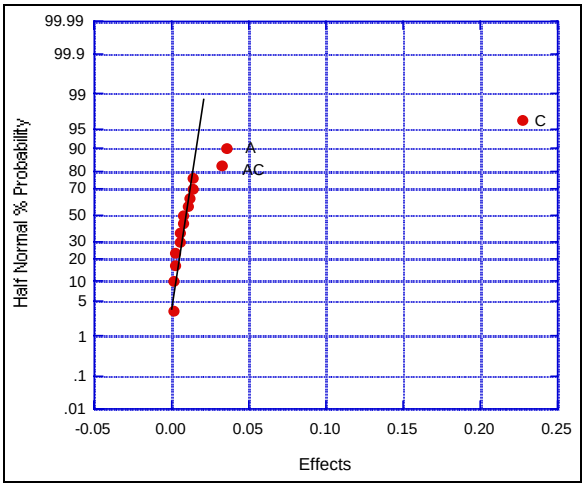

Figure 5.-Factor Effects Plot for Offset Voltage

used later is plotted similarly except using the actual value of the factor effect instead of the absolute value. Those factors which have trivial effect will scatter normally with small deviations about a straight line, while the factor effects calculated from the statistically significant factors will show a large deviation from the line. As expected, the zero offset voltage V_0 is highly dependent on the module temperature (A), the module range (C) and an

interaction of these two factors labeled AC. The V_0 regression model is shown in Equation 4.

$$V_0 = \beta_0 + \beta_A A + \beta_C C + \beta_{AC} AC + \in \quad (4)$$

The insignificant factor effects (those close to the line) become a part of the system error ($\in$) in equation 4.

Similarly, responses A_1 and A_2, the low pressure characterization coefficients, and A_4, the nonlinearity coefficient, depend on pressure direction "B", module range "C", and an interaction of these two factors "BC" as shown in Figure 6a-6c. These figures are normal effects plots which were discussed previously. Equation 5 shows the regression equation for coefficients A_1, A_2, and A_4, noting that the β values will be different for each case.

$$A_i = \beta_0 + \beta_B B + \beta_C C + \beta_{BC} BC + \in \quad (5)$$

where, I = 1, 2, or 4.

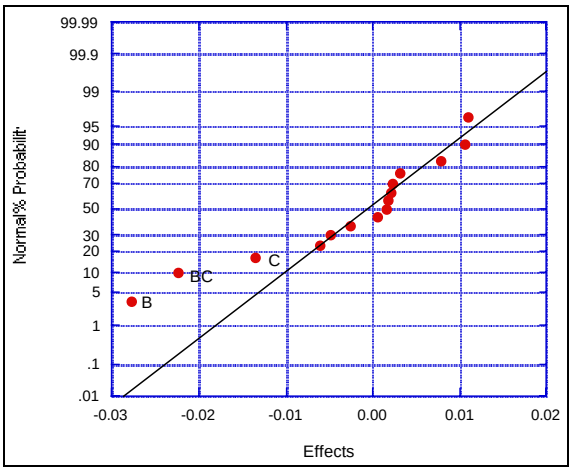

Figure 6a.-Factor Effects Plot for A1 Coefficient

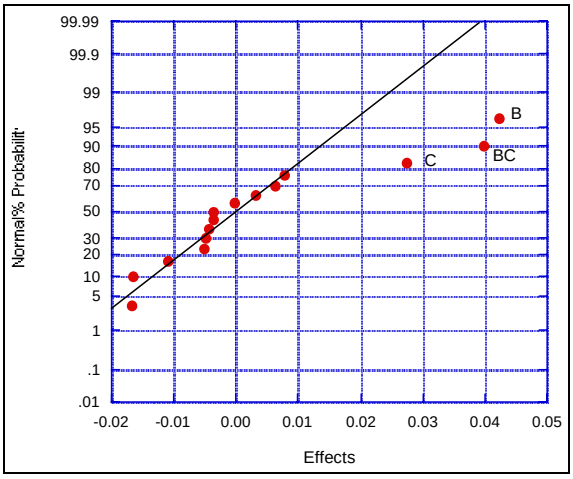

Figure 6b.-Factor Effects Plot for A_2 Coefficient

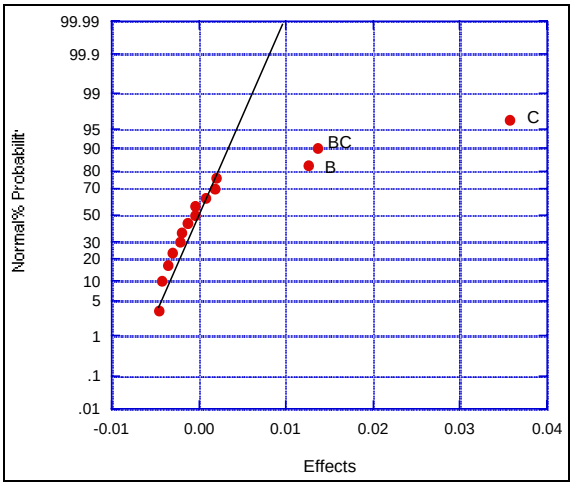

Figure 6c.-Factor Effects Plot for A4 Coefficient

A_3, the slope sensitivity coefficient is shown in Figure 7. It depends on the module range alone, as expected from experience. The defining regression model is shown in equation 6.

$$A_3 = \beta_0 + \beta_C C + \in \quad (6)$$

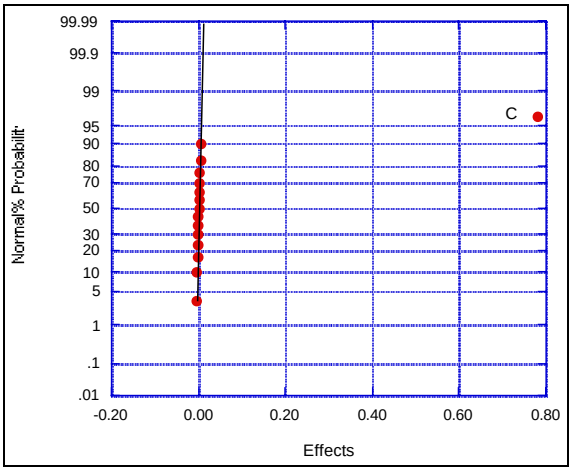

Figure 7.-Factor Effects Plot for A3 Coefficient

Sample rate and sample period never appeared as possible significant environmental factors during the Phase I DOE study. However, since vibration effects were not considered, it is possible that the interaction between vibration and sample rate or sample period may be significant. Therefore, they will be retained during the Phase III analysis. The Phase I test provided an independent verification of the low-pressure response characteristics described by Everhart. Figure 8, which is similar to Figures 2a and 2b, shows the knee region that all ESP transducers appear to have.

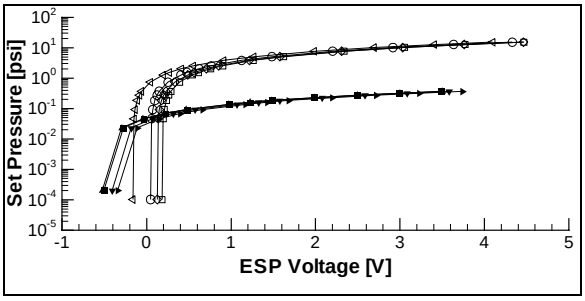

Figure 8.-Phase I: Pressure vs. Voltage Plot

Phase II- Calibration Stability and Constraints

Phase I provided an abbreviated subset of the available factors that potentially affect ESP uncertainty and some of the interaction effects among those factors. Phase I also provided independent verification of the calibration improvements proposed by Everhart (1996). Experience gained in Phase I emphasized the need for better control of low pressure conditions. Therefore, the development of a full DOE experiment was initiated. The first requirement that must be satisfied prior to any DOE testing is the existence of a predictable experimental process. This means the process must be in statistical control and defined prior to actively inducing measurement variation. SPC is being used to assess the predictability of the ESP measurement systems and the ESP transducer calibration coefficients over time to determine if they stay in statistical control with the testing conditions held constant. Once a predictable calibration system is achieved, randomization of set point order, vibration, and IFC configuration study will be conducted using DOE or SPC methods to determine if any of these factors provide a significant change in the voltages measured and hence a change in the calculated calibration curve coefficients. These studies will provide knowledge of system constraints which will aid the development of test procedures in which the Phase III experimentation will be conducted.

Shewhart, the father of the 3 sigma control chart, defined statistical control by stating: "A phenomenon will be said to be controlled when, through the use of past experience, we can predict, at least within limits, how the phenomenon may behave in the future" (Shewhart, 1980). SPC uses Shewhart's control charts to detect the presence of uncontrolled variations. Once an uncontrolled variation is detected, the process can be studied to determine the existence of an assignable cause or source of the disturbance. Once identified, a solution for the problem can be developed.

The first step in applying SPC is to develop a control chart for individual measurements in a process. This chart is created by plotting the individual values (X) relative to the time order of acquisition (index) seen in chart titled, "A_1 Coefficient" in Figure 9. Actual Data for this chart were obtained in a 9-run SPC study that was conducted at the beginning of Phase II and will be used as an illustrative example. SPC uses the moving range of adjacent data points to develop an estimate of the standard deviation. A Range chart, which is titled, "A1 Moving Range" in Figure 9, is created by plotting the

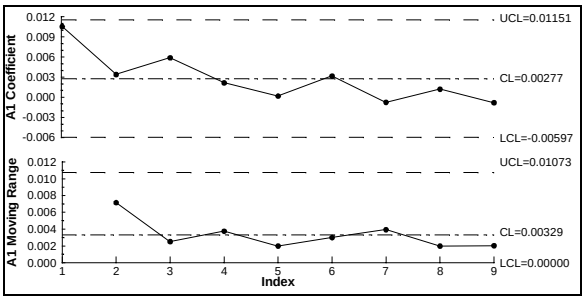

Figure 9.-A_1 SPC Control Chart

calculated moving range values (R), which are always positive, relative to the same index. Once these charts are plotted, process means ($\overline{X}$), Mean Range (R), and upper and lower control limits (UCL and LCL) are calculated and drawn on each chart. The calculations used to create the individuals control charts are relatively easy to calculate as seen below in equation 7.

$$\begin{aligned} (U \text{ and } L)CL_X &= \overline{X} \pm A_2 \overline{R} \\ CL_X &= \overline{X} \\ R &= X_{i+1} - X_i \end{aligned} \qquad (7)$$

where:

$\overline{X}$ is the average of the data and A_2 is found in table A-2 of Wheeler, 1984.

The A_1 coefficient lies between the upper and lower control limits, indicating that the system is in control. However, the consistent downward trend in the individuals chart is indicative of a changing system. A predictable system should vary randomly about the process mean labeled as CL in the A_1 coefficient plot. According to SPC rules, the A_1 coefficient is marginally out of control. Points that are clearly out of control are found outside the control limits, although, there are other detection rules that signal significant changes in the system.

There are possibly multiple causes for the unstable behavior seen in Figure 9 due to test procedures, operator error, or lack of environmental control, all of which illustrates the need for an automated and tightly defined control and testing procedure. To provide this tight control, an automated calibration and data acquisition system was developed by

modifying an existing calibration system to have the capacity to set pressures for long periods and over the full range of ESP modules that are in use in the Langley hypersonic wind tunnels. LabVIEW programming was used to provide tight procedural controls for the data acquisition, environmental, and calibration pressure control system. The environmental pressure is provided and maintained using a specially constructed pressure vessel shown in Figure 10 which will be referred to as the Environmental Control Chamber (ECC). The ECC and calibration control system design, construction, and predictability testing will be discussed further in the calibration control system section of this paper.

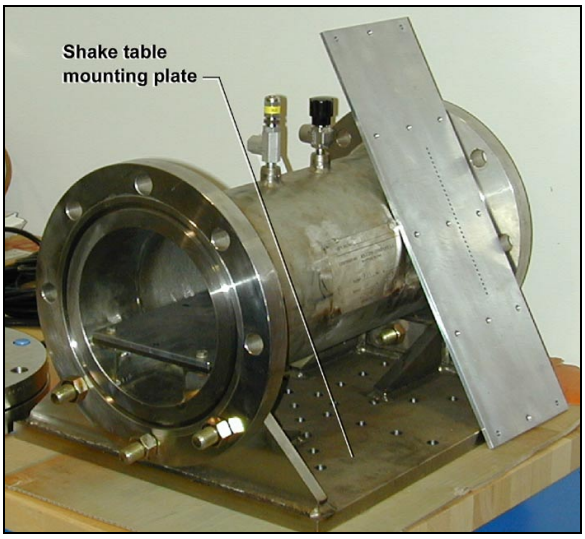

Figure 10.-Environmental Control Chamber

Phase III- Full Screening Experiment

Phase III consists of a multi-factored 2-level fractional factorial screening design. The eight factors considered at this time are: sample rate, sample period, settling time, module range, module temperature, vibration, vibration direction, and environmental pressure. Each factor will be tested at two levels having a high and a low value. Analysis of variance methods will provide a regression model solution for the system. This description will provide identification and quantification of factors and factor interactions that significantly contribute to measurement error. The significant factor identification will lead to implementation of appropriate environmental controls of significant factors and interactions, thereby lowering the uncertainty and increasing accuracy of ESP transducer measurements in hypersonic wind tunnels.

Calibration Control System

Due to the lack of predictability found in first study of Phase II, an automated calibration control system was designed and constructed to set, control, and accurately measure pressures. The calibration control system (Figure 11) consists of an MKS 146C PID pressure controller, 1-psid and 15-psid Ruska pressure transducers, Hastings Gauge (HG) reference pressure gauge, two Varian turbo vacuum pumps (TP), LabVIEW programmed data acquisition computer (DAQ), and a National Instruments SCXI

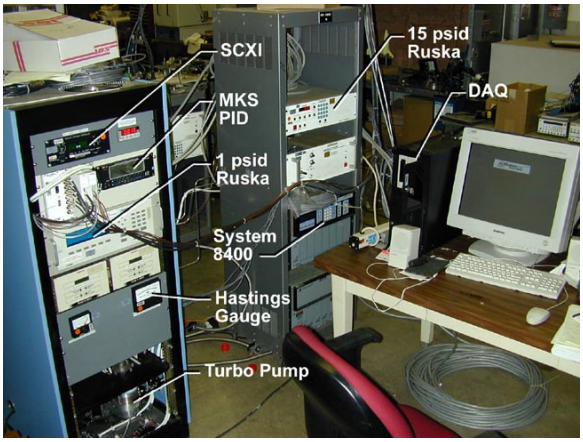

Figure 11.-Calibration Control System

chassis (SCXI). These system components will be discussed further future sections.

Environmental Control Chamber

Due to the sensitivity of ESP transducers to temperature, pressure, and vibration, an environmental control chamber (ECC) was designed to house up to four ESP modules seen in Figure 12 and the Interface Controller (IFC), through which the ESP module measurements are multiplexed. Pressures in the ECC can be set as high as 135 psig with temperatures up to 200º F. The ECC was constructed so that it can be mounted to a shake table allowing vibration error characterization. Pressure, thermocouple, and signal wires are fed through the ECC flange through the use of bulkhead connectors to provide for the transfer of pressure and heater voltage into the ECC as well as to transfer

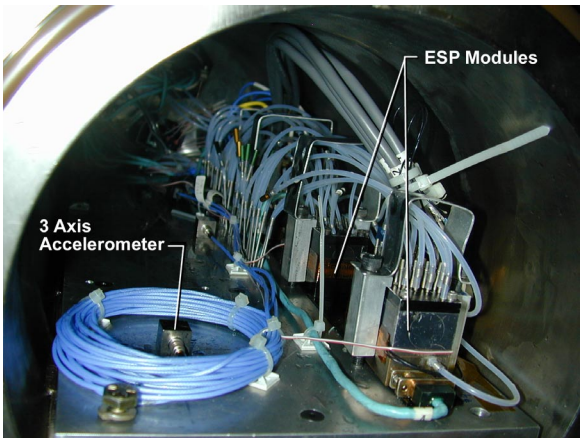

Figure 12.-ESPs Inside the ECC

temperature, acceleration, and pressure transducer signals out of the ECC (Figure 13). Cables were also

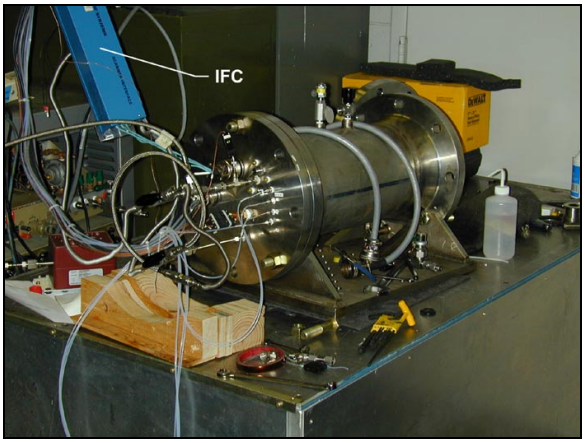

Figure 13.- ECC Pressure & Signal Connections

constructed to allow the IFC to be reconfigured inside or outside the ECC depending on test conditions. A pressure manifold mounted within the ECC allows up to 32 pressure ports to be connected to a common pressure source (Figure 14).

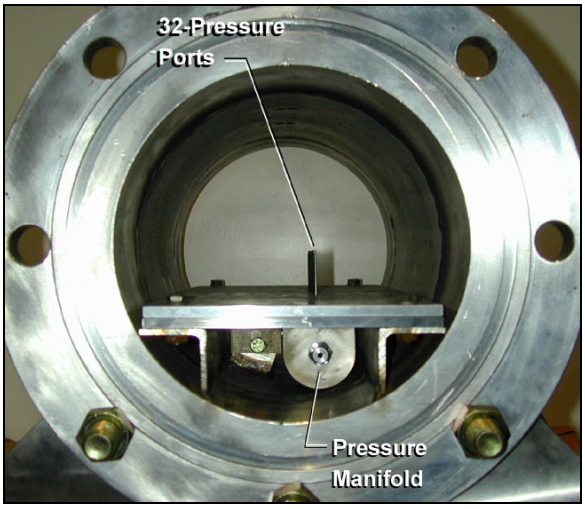

Figure 14.-EEC Pressure Manifold

This manifold also helps to stabilize the mounting platform within the ECC when it is vibrated normal to the platform.

Pressure Control System

An existing dead-end low pressure calibration system originally designed to be a similar to the how the MKS cart was used in the Phase I test was modified by adding an MKS Proportional Integration Derivative (PID) controller, to control the ESP calibration pressures (Figure 15). This PID controller drives a proportioning valve (PV), providing a controlled leak, and thereby enabling pressures to be set and held over long durations. This capability allows for the long settling times required for low pressure calibrations.

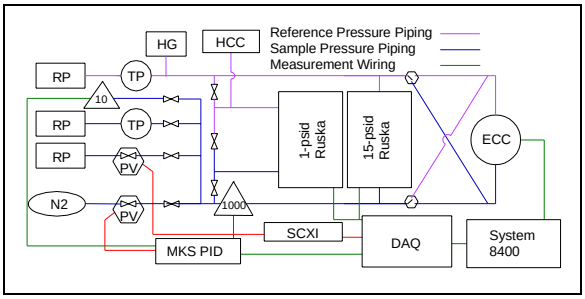

Figure 15.-Calibration System Diagram

The ESP modules, mounted inside the ECC are connected to the System 8400, have pressure ranges from 0.36 to 15 psid. Continuous setting of differential pressure from as low as 0.001 psid and up to 15 psid is required to calibrate modules of these ranges. This wide pressure range is difficult to precisely control. The proportioning valve must be sized to set the very low pressures with high vacuum, while the high pressures require low vacuum and a large orifice proportioning valve. To solve this problem a large orifice proportioning valve (PV) was used to throttle the vacuum pump. This valve was indirectly controlled by the DAQ, through the National Instruments SCXI chassis (SCXI). The Turbo vacuum pumps (TP) were used to achieve very high vacuum levels ($<10^{-4}$ Torr). A valve controlled by the DAQ is provided to isolate the turbo vacuum pump so that the system pressure can be raised. This allows pressures to be set from 0.001 to 15 psid if the system input pressure is 16 psia is provided at the point denoted N2. Currently, the system does not have an input pressure above atmospheric pressure so the highest controlled pressure that can be set is approximately 12.5 psid. Atmospheric pressure can be set by eliminating the vacuum sources and opening the proportioning valve. Zero pressure is obtained by equalizing the calibration and sample lines and sliding the ESP calibration block to the calibration position to shunt the reference pressure to both sides of the transducer.

The PID controller can set and hold pressures above zero within two percent of the set point. Stability of the controlled pressure is increased by the ECC pressure manifold and 25 feet of stainless steel pressure transmission tube. This dampens small pressure fluctuations and further stabilizes pressures seen at the ESP modules. This stability can be seen in the sample data shown in Figure 16. The pressure is transitioning from the previous set point to the new set point. The Ruska Pressure Chart on the top shows the out of control system settling into control as the PID Pressure Chart on the bottom shows the natural cyclic control being applied to the system. Note the control limit labels in both plots. The range in the Ruska Chart between the control limits is 0.00095, while the range in the PID Chart is 0.00597,

illustrating an order of magnitude increase in pressure stability over a 200 second time period.

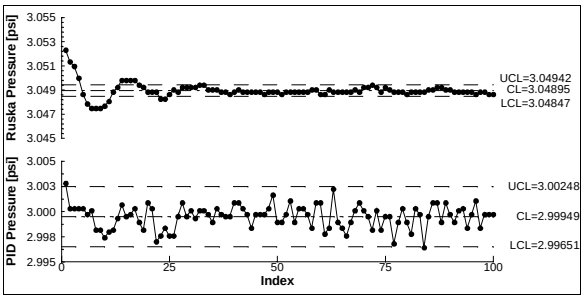

Figure 16.-Sample Stabilization Data

Control Pressure Measurement

High accuracy pressure standards made by Ruska are used to provide a stable pressure reference and to independently monitor the calibration pressures provided by the newly added MKS PID pressure control system. The calibration pressures are measured by two Ruska quartz bourdon tube differential gages. Pressures below 0.9 psid are measured by a Ruska 7000 1-psid transducer and pressures above 0.9 psid are measured by a Ruska 6000 15-psid transducer (Figure 15). These Ruska devices are an order of magnitude more accurate than the PSI pressure control unit with much less drift over time. A National Institute of Standards and Technology (NIST) traceable calibration was conducted prior to testing and verified that the accuracy of both Ruska transducers fall within the ±0.010% of reading ± 0.003% of full scale specifications, while the PSI pressure control unit has a specified accuracy of 0.02% of full scale.

Because of the independent measurement and control systems, SPC analysis of the ESP voltage measurement system will be difficult due to drift in the pressure control manometers. The set pressure may fluctuate due to PID manometer drift; however, the control pressure measurement system will detect any drift and account for changes in the pressure difference measured by the Ruskas. To minimize drift in the Ruska standards, it is essential that they are not over pressurized during the course of an experiment. Therefore, both hardware and software protections are provided for the 1-psid gage to ensure over-pressurization of the Ruska standard does not occur.

Temperature Data Acquisition

Temperature gradients are symptomatic of pressure gradients in the system. Accordingly, air temperature is measured at the pressure manifold inside the ECC, at the reference pressure feed-through just outside the ECC, and as near as possible to each Ruska standard's sample and reference ports. These temperatures are measured to verify that the relative air temperature between ESP transducer and the Ruska standards have not significantly changed during the course of setting pressures. Due to the stability of the reference pressure and lack of available channel on the isolation amplifier in the SCXI chassis, the three reference measurements are acquired through the data acquisition card that doesn't have a terminal temperature reference, thereby lowering the accuracy of these measurements. These low accuracy measurements are acquired near the ECC and the Ruska standards only to look at relative temperature differences that may be found in the reference pressure transmission line, which should rarely change because of the consistent low pressure being held.

Temperature Control

Module temperatures are also acquired through the SCXI and used to determine the amount of heater time required to keep the module at the set control temperature. A LabVIEW software PID controller is used to determine the required heater time. The DAQ acquires 20 samples from each port at 40 samples per second and filters the data by calculating the RMS value for each channel. The filtered data is input into the PID controller and the temperature is maintained to within 0.1º F of the set temperature.

Error Minimization

The calibration system is large with long data cables and pressure transmission lines. Shielded cables were used to protect data transfer with careful attention directed toward eliminating ground loops. DC control voltages were used where possible to minimize the signal contamination. Where AC control voltages are used, signal cables were separated as much as possible. Pressure transmission lines used O-ring connections to minimize vacuum leaks. Within the pressure control rack crush ring connections are used to virtually eliminate vacuum leaks. Crush ring connections were used in connections that do not need to be disconnected for system relocation. The largest vacuum leaks were found within the ESP modules themselves. These leaks are controlled by placing the ESP modules in a vacuum environment which is one of the control factors to be tested in Phase III. Reducing the pressure within the ECC to a moderate vacuum eliminates the ESP module leaks by lowering the differential pressure between the environment outside ESP module and the control and reference pressures provided inside the module.

System Capabilities

The calibration control system was designed to enable high accuracy calibrations for ESP transducers. Simulated differential calibrations can be conducted by crossing the sample and reference pressure transmission lines using three-way valves (Figure 15). This procedure allows the sample

pressure to be channeled to the reference side of the ESP transducer and the reference pressure to the sample side. Currently, true differential calibrations can be conducted for 5 psid modules and below due to the control span of the calibration system. However, an external pressure source must supply the ESP modules a statistically controlled reference pressure.

System Calibration

The process of quantifying the capabilities of the calibration system requires the characterization of two control subsystems, which are the temperature control and pressure control, and the control-dependant transducer measurement system. Each subsystem will be evaluated to determine the stability of the control. The transducer measurement system will then be analyzed with control subsystems being employed.

Calibration Sequence
Each calibration run consists of nine pressure set points that are each controlled, and measured for 45 minutes. Once 45 minutes of data is taken at a sample rate of one measurement data set every two seconds, the system moves to the next set pressure and system repeats itself. The set point pressures for each run are found in Table 1.

Run Set Pressures		
Point	Psid	Torr
1	0.0000	0.000
2	0.0010	0.052
3	0.0100	0.517
4	0.0330	1.707
5	0.1000	5.172
6	0.3300	17.066
7	1.0000	51.715
8	3.0000	155.145
9	5.0000	258.575

Table 1 Calibration Point Pressures

After initialization to configure control valves, the system is started, file paths are set, the ESP system is reset then initialized, the calibration blocks are slid to their required positions, and the ESP data acquisition is triggered. Data acquisition is begun before the pressure is set to gain settling time information for each set pressure. Temperature, pressure, and ESP voltage data are acquired every two seconds. Each Transducer voltage data point consists of an average of 10 measurement scans taken with no delay between frames. The ESP voltage data are acquired and stored within the System 8400 until the end of acquisition when they are transmitted to the DAQ and written to file. After completion of each calibration point, the system loops back to set the start point until all calibration points have been acquired. Then the system turns the temperature control off and pumps the whole system to a hard vacuum to prepare for the next run. If auto restart is on, the system will wait until the reference pressure is below 8.7×10^{-6} psi and module temperatures fall to a level 5 degrees below the temperature set point, then the system will restart and repeat the calibration run with an updated run number.

Temperature Control
Type J thermocouples are used to measure the ESP module temperature. Bonding material on the type J thermocouples used will not allow a NIST traceable calibration to be performed prior to the experimentation. Therefore, a sample set of data was taken over a 10 second period at 20 KHz to determine the statistics for each thermocouple. The sample means and standard deviations were used to ensure that the three sigma precision of the thermocouples fell within the specified error bounds set by the manufacturer. The raw temperature data varied from normality as shown in normal probability plot in Figure 17, where the straight line represents

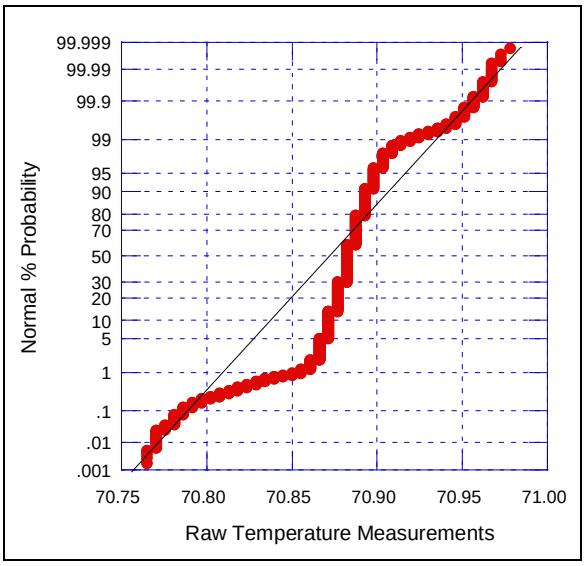

Figure 17.-Raw Temperature Measurement

the Gaussian or Normal distribution. To increase the stability of the temperature measurements, the RMS value of 20 samples was calculated and used as the transducer temperature, thereby filtering the measurements. This filtering was conducted to reduce the noise found in the temperature measurements. Figure 18 shows the filtered data that generally plots as a straight line. Because the thermocouples bonding material would be destroyed by the calibration procedure, the bias between a NIST traceable standard and the thermocouples will be determined after the completion of the experimentation. This will only be needed for anecdotal reasons because no comparisons will be made between modules based on temperature equality.

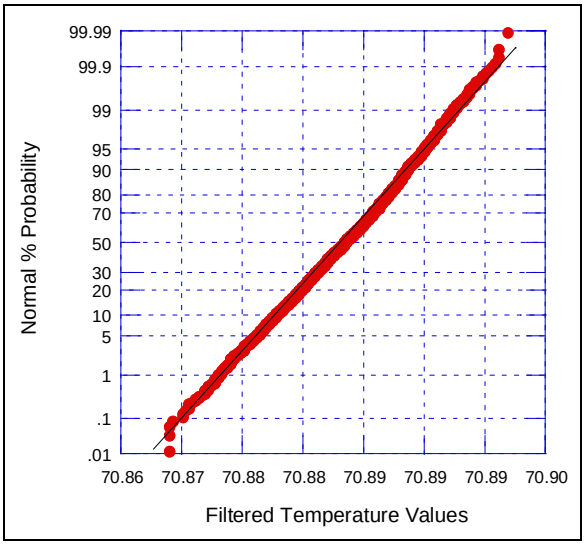

Figure 18.-Filtered Temperature Values

The module temperature control system has also been analyzed using SPC to verify that the temperatures are maintained at the set temperature in a controlled manner. Looking at the control charts in Figure 19, there are some temperatures that fall outside the control limits. In large data sets it is common to see an occasional outlier; however, these occur at more than 1% of the indices and do not correlate with the three sigma control limits which allow 1 outlier per 100 points (Note that each index accounts for 2 seconds of time). However, the temperatures are being controlled predictably to well within 0.1º F.

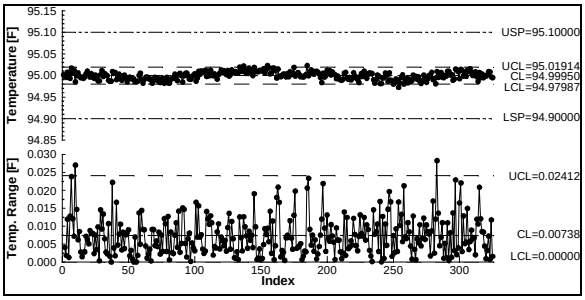

Figure 19.-Temperature Controllability Chart

Pressure Control

The PID manufacturer has no specification for pressure control ability. A PID controller is limited only by input measurement accuracy and tuning. To limit control problems, the pressure measurement system (the Ruskas) is independent of the pressure control system. Therefore, the measured differential pressure may or may not be similar to the set pressure. At higher pressures, the pressure control system provides enough variation in the measured values that control limits can be calculated (Figure 20). However, the measurements are approaching the instrument resolution with only three discrete range values calculated within the moving range limits, the individuals' control chart limits are distorted and

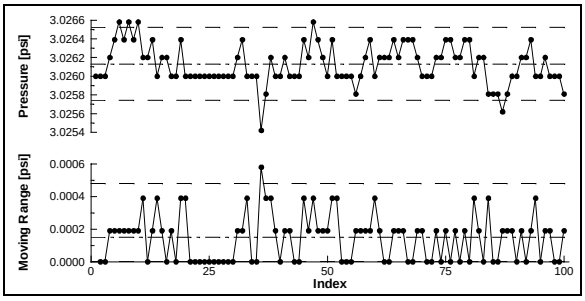

Figure 20.-High Pressure Controllability Chart

depict the system as being out of control when it is not. Wheeler (1995) describes this phenomenon in section 5.6. Figure 21 shows the pressure settling near the end of observable variation. The measured pressures from the 1 psid Ruska are very stable over time in the very low pressure regime due to the pressure control system stability. The measured pressures shown in the pressure individuals chart in Figure 21 are so consistent that control limits cannot be calculated due to the lack of resolution found in the Ruska which is illustrated by the consistent zero moving range values. Therefore, in both situations, the calibration pressures are set and held stable in a statistically controlled manner.

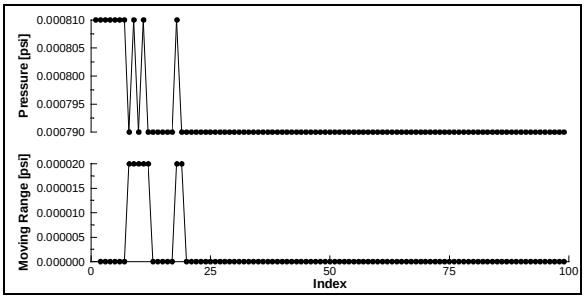

Figure 21.-Low Pressure Controllability Chart

ESP Voltage Measurements

Silicon diaphragm transducer voltage measurements are sensitive to temperature and pressure changes. As a result, these factors must be controlled to determine the stability of the voltage measurements. Using the temperature and pressure controls discussed above, the voltage data can be acquired at each set pressure holding the temperature constant at 95º Fahrenheit. A sample of the acquired ESP transducer voltage, temperature, and calibration pressure data from calibration run 3 during set point 2 is shown in Figure 22.

The three individuals' charts in Figure 22 show the voltage acquisition is started prior to the pressure being set near index 5, allowing the viewer to see the system response and the pressure settle over time (measurements are acquired every two seconds). Notice the set pressure (bottom) settles faster than the transducer voltage. At low pressures, the transducer voltage requires a very long time to settle near 45

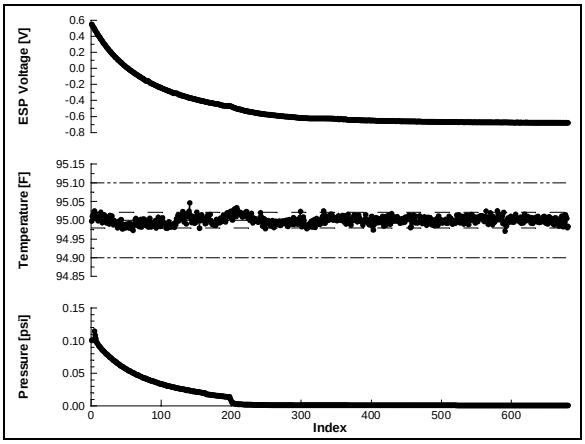

Figure 22.-Sample Calibration Data

minutes. However, it is arguable that the 45 minutes of settling is not long enough to achieve stability at very low pressures. Figure 23 is a close up look of

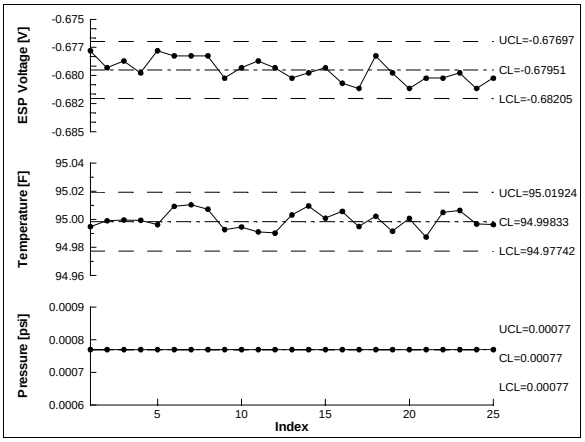

Figure 23.-Close-up of Sample Calibration Data

the last 25 measurements acquired at set point number 1. Note that the voltage (top), temperature (middle), and pressure data (bottom) are all within the control limits, indicating a stable system. However, the ESP voltage plot still has a downward trend and may not be totally settled. At higher pressures settling time is less as shown in Figure 24 for set point 7. Note how quickly the pressure stabilizes.

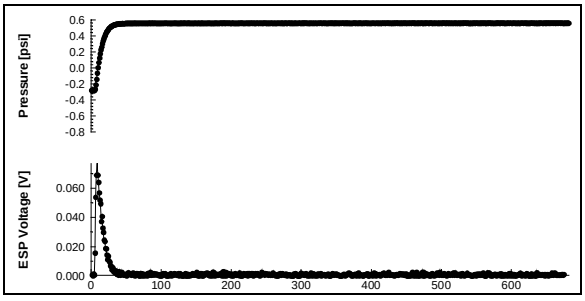

Figure 24.-Sample High Pressure Calibration Data

Repeatability

The repeatability of each data point is important for calibration accuracy over time. Note a point refers to a pressure setting during a given run. Figure 25 is a three-way chart used as an illustrative example to analyze the repeatability of set point 2. This chart

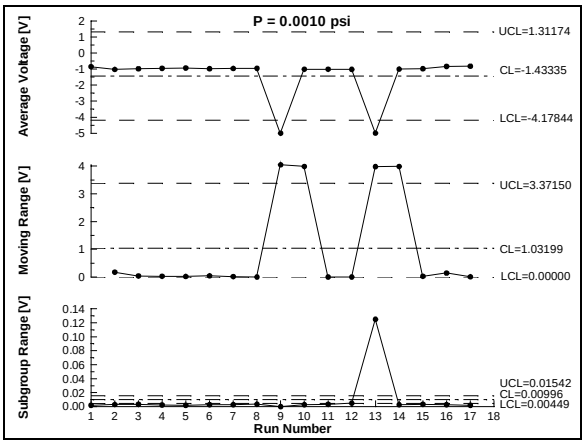

Figure 25.-Raw Repeatability Data for point 2

compares relative values from each run and highlights the second level of variation in a process. It, also, shows the level of repeatability between averaged subsets. The Average Voltage Chart (top) is plotted similarly to the individuals chart, except using the subgroup averages ($\overline{X}$) calculated from the last 24 measurements obtained at the prescribed set point during each run. Therefore, each plotted point on averages chart is the average settled value calculated for each run. The Averages Chart is used to determine whether the system is operating in a statistically controlled manner. The Range Chart (bottom) is plotted using the range of the values found *within* the subgroup and illustrates the relative run to run variation in the subgroup data. The Moving Range Chart (Middle) is generated using the calculated moving range (R) of the subgroup averages ($\overline{X}$) and is used to assess *between* group variation and to determine the control limits for the Average Chart. The equations for these calculations are found in Wheeler (1984) and are presented in Equation 8.

$$
\begin{aligned}
&U \text{ and } L\ CL_{\overline{X}} = \overline{\overline{X}} \pm A_2 \overline{R} \\
&CL_{\overline{X}} = \overline{\overline{X}} \\
&UCL_R = D_4 \overline{R} \\
&CL_R = \overline{R} \\
&LCL_R = D_3 \overline{R} \\
&R = \overline{X}\, i{+}1 - \overline{X}\, i
\end{aligned}
\qquad (8)
$$

where:

$\overline{X}$ is the sample average, $\overline{\overline{X}}$ is the average of $\overline{X}$, $\overline{R}$ is the average of R, and A_2, D_3, D_4 are found in table A-2 of Wheeler, 1984.

Figure 25 shows a process that appears to be out of statistical control because of points outside of the control limits. SPC declares that a problem doesn't exist unless it is identified in a control chart. Once a problem is identified, further investigation of the individual out-of-control point is conducted to determine the assignable cause. If an assignable cause is identified, only then can the point be rejected. It is obvious that some of the points in the system are bad and should be removed.

Data Runs 9 and 13 in Figure 25 were found to be corrupted, due to the communications problems within the ESP measurement system. With these corrupt points removed, Figure 26 shows filtered repeatability data with new calculated limits that show that runs 1, 11, 14, and 15 are of interest due to points falling outside the control limits on either of the charts. Between runs 13 and 14 ESP

System data-cable connections were found to be loose and tightened, thereby, possibly causing a change in the system. Loose data cables may cause higher resistances at a connection which can shifted the mean transducer voltage measured. With further

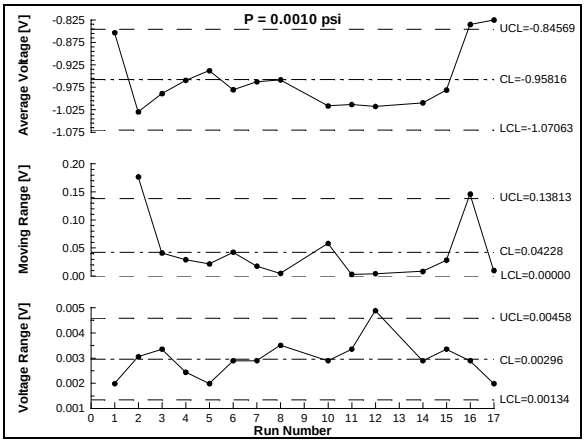

Figure 26.-Filtered Once Repeatability Data

testing it is possible to determine if the true mean is found in the -0.83 volt region or whether it, indeed lies near the -0.0958 centerline. To further analyze the repeatability of the system, an assumption is made that the loose cable caused runs 1, 14, and 15 to shift. It is assumed that removing these data points will show the system is operating at the same conditions. Therefore, these data are removed for the purposes of further analysis. Run 11 was examined to determine why its subgroup range was elevated. No reason was determined to account for the elevated range, however, with run 1, 14, and 15 removed and limits recalculated; point 11 is only marginally out of range and is included in Figure 27. Figure 27 describes a system that is only marginally in control because the data do not randomly scatter around the mean value as discussed in section 5.7 of Wheeler, 1995.

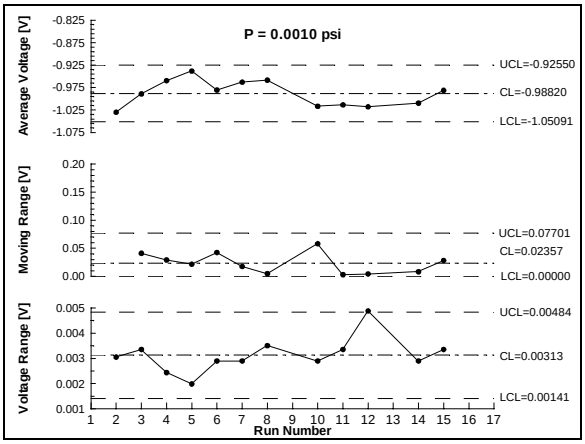

Figure 27.-Final Filtered Data

Figure 28 shows the average voltage charts of all of the set pressures denoted by point number given in Table 1. The numbers of data points differ because of the intermittent communication problems discussed previously. Charts for Points 1 through 6 were taken from a .36-psid module. Notice the similarities of the point 1 through point 5 Average Charts and the difference between them and the Point 6 average chart. The similarities of the first five charts are likely to due to the 10 Torr manometer drift and the reference pressure. However, the reference pressure shown in Figure 29 shows that the average ESP voltage is very similar to the reference pressure that is measured by a Hasting Gauge (HG) Figure 15. The Hasting gauge provides a nonlinear output voltage that is monitored by the DAQ and used to create Figure 29. Only two programmatic differences are known to change between these two points and are the most probable causes of the differences between point 5 and 6. These are the tuning parameters and control manometer used by the PID controller. The tuning parameters are used to direct the PID controller's actions. The parallel behavior between ESP Voltage and the measured pressure in Figure 30 illustrates that the 1000-Torr manometer drift is causing a large portion of the variations found in the Control Charts for point 6.

Points 7 thru 9 charts illustrate the voltage measured from a 15-psid transducer. Manometer drift may partially account for some run to run variation as it did in set point 6, however, the large chart to chart inconsistencies seen in points 7, 8, and 9 of Figure 28 are due to tuning parameters for the PID controller. Tuning parameters in general are pressure dependant and need to be tuned differently for each prescribed pressure range. Currently, only one set of tuning parameters are configured for the 1 to 15 psid range.

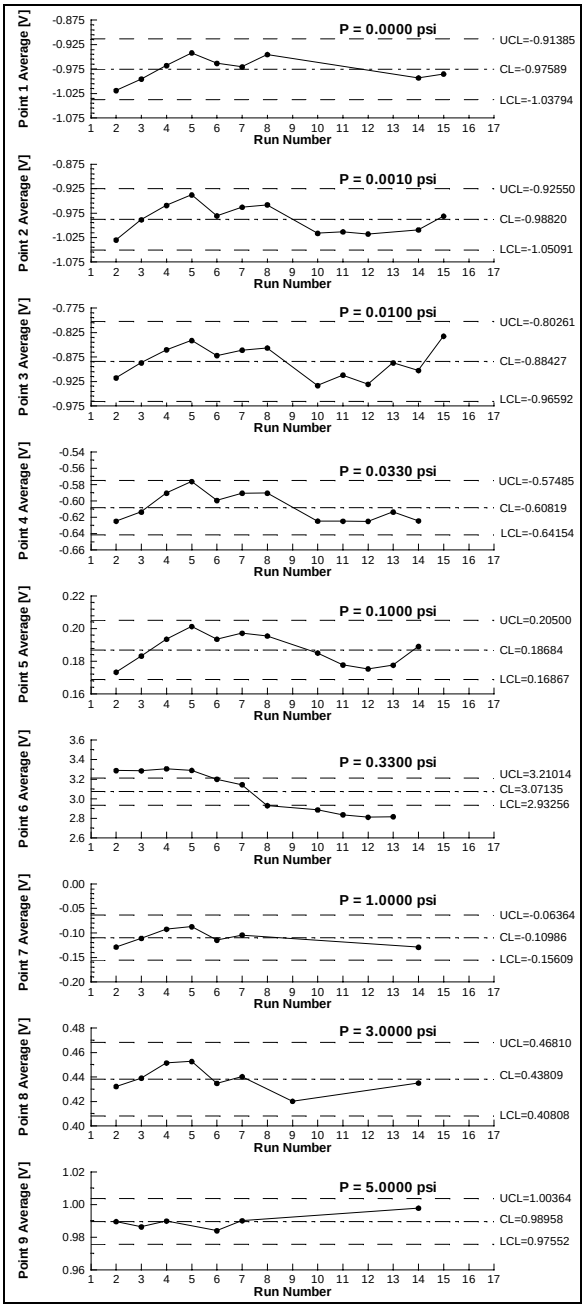

Figure 28.-Filtered Repeatability Data

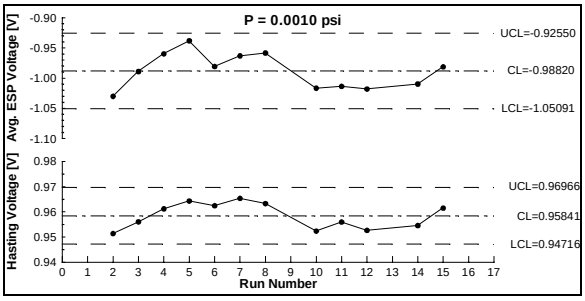

Figure 29.-ESP and Hasting Voltage Comparison

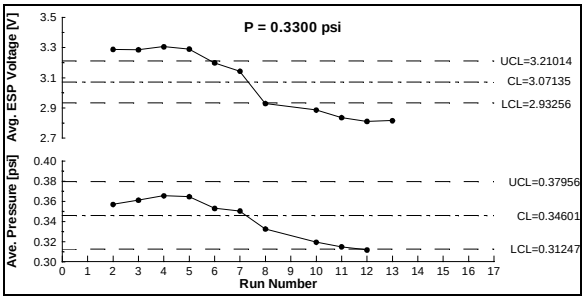

Figure 30.-Pressure Voltage Comparison

Discussion

The calibration control system has demonstrated that pressures are being held precisely over long time periods and within the measurement resolution of the Ruska standards in the low pressure regime. More pressure variation is seen at higher pressures, even though pressure variations are held near the measurement resolution of the standards. Variations seen are most likely being caused by the broad use of a single set of tuning parameters in the PID controller. Additional sets of tuning parameters are required over the 14 psi range controlled by the 1000 Torr manometer, since tuning parameters are pressure dependant.

Further system tuning is required prior to using this system for environmental characterization due to a lack of run to run repeatability. The limits on the ESP voltage 3-way control chart must be narrowed to provide the ability to statistically differentiate between very low pressures set by the pressure control system. Currently, the set point 1 voltages (0.0000 psid) are indistinguishable from the voltages seen in set point 2 (0.001 psid) as shown in Figure 28. Set Point 3 (0.01 psid) control limits overlap into the range of set point 1. These control limits can be narrowed by reprogramming the calibration system to measure the offset pressure between the control manometers and the Ruska standards, then adjusting the pressure set point which will reduce the drift variation to that of the Ruska standards. Reference pressures must also be monitored closely to verify that reference pressures are held in a consistent manner while repeatability and calibration data are being acquired.

The temperature control has been tested and determined to be only marginally out of statistical control, but well within the required specifications. The control temperature is being held to within ±0.1°F, an order of magnitude tighter tolerance than the manufacturers off-the-shelf temperature control box which hold temperatures to within ±1° F. To obtain tight statistical control, further testing will be conducted looking at the PID tuning parameters to determine if the current cyclic control variations seen in Figure 19 can be minimized.

Concluding Remarks

The characterization of environmental error of LaRC wind tunnel ESP measurement systems required that a simulation test bed be constructed with similar instrumentation and pressure transmission dimensions found in the hypersonic laboratory wind tunnels. The calibration system is different from the hypersonic wind tunnels in that the ESP's calibration pressure control and measurement system is bypassed to enable the use of higher accuracy pressure controls and reference standard s.

With additional tuning, these systems have the potential to increase calibration stability and should provide the ability to statistically differentiate between very low pressure measurements (i.e. those currently below the specified range of the ESP transducer). It will, also, allow repeated calibrations to be conducted over time, generating statistically predictable calibration coefficients. Environmental and procedural controls can, then, be applied to enhance ESP transducers calibration stability. Potentially, this will reduce the calibration frequency to the order of a wind tunnel test, saving time and resources.

The calibration control system is not yet functioning at the levels of repeatability required to distinguish between very low pressures. Control manometer drift, reference pressure fluctuations, and incorrect use of tuning parameters are possible sources of the added variability found in the ESP transducer response voltages. Software changes will provide well tuned and properly applied tuning parameters, manometer drift reduction to that of the Ruska standard drift specifications, and in-process reference pressure verification to ensure stable reference pressures. Further investigation and system tuning must be accomplished prior to progressing with the residual Phase II and III studies. Once the calibration process is repeatable in statistically controlled manner, SPC will be used as an ongoing assessment of the process to monitor the system stability.

Acknowledgments

The author would like to thank Anthony W. Robbins of Aerothermodynamics Support Section, Gas, Fluid, and Acoustic Research Support Branch, Aerodynamics, Aerothermodynamics, & Acoustics Competency, NASA Langley Research Center) for his technical knowledge of instrumentation systems used in hypersonic wind tunnels and for his enthusiasm and expertise in constructing the high vacuum constrained calibration control system.

References

Everhart, Joel L. 1996: "Calibration Improvements to Electronically-Scanned Pressure Systems and Preliminary Statistical Assessment", AIAA Paper No. 96-2217.

Shewhart, Walter, (1931): "Economic Control of Quality of Manufactured Product", republished by American Society for Quality Control, Milwaukee, Wisconsin, 1980

Stat-Ease, Inc. 2002: "Design Expert", Version 6.0.6, Stat-Ease, Inc., Minneapolis, MN

System 8400 User's Manual CD, Pressure Systems Inc., Hampton, VA, 2002

Montgomery, Douglas C 1997: 'Design and Analysis of Experiments", 5th Edition, John Wiley& Sons, Inc., New York, NY.

Myers, Raymond H.; and Montgomery Douglas C. 2002: "Response Surface Methodology", Second Addition, John Wiley& Sons, Inc., New York, NY.

Operation Manual for Mensor Digital Pressure Gauge Model 11900. Manual Part Number 11840-001; 500; 10/81, Mensor Corporation, San Marcos, Texas, Oct. 1981

Wheeler, Donald J.; and, Chambers, David S. 1992: "Understanding Statistical Process Control", Second Addition, SPC Press, Knoxville, TN.

Wheeler, Donald J.; and Lyday, Richard W. 1984: "Evaluating the Measurement Process", Second Addition, SPC Press, Knoxville, TN.

Wheeler, Donald J. 1995: "Advanced Topics in Statistical Process Control", SPC Press, Knoxville, TN.